A powerful new technology platform to address new R&D strategies in timing sensor technologies: When silicon technology meets ultrafast lasers at ELI

<u>Gordana Lastovicka-Medin</u>
University of Montenegro

Gregor Kramberger
Jozef Stefan Institute

Mateusz Rebarz, Jakob Andreasson, Kamil Kropielniczki
ELI Beamlines

Jiří Kroll, Michal Tomášek, Marcela Mikestikova, Tomáš Laštovička
Institute of Physics, Academy of Sciences, CZ

Valentina Sola Nicolo Cartiglia
INFN Torino

International Workshop on Future Linear Colliders, LCWS2021

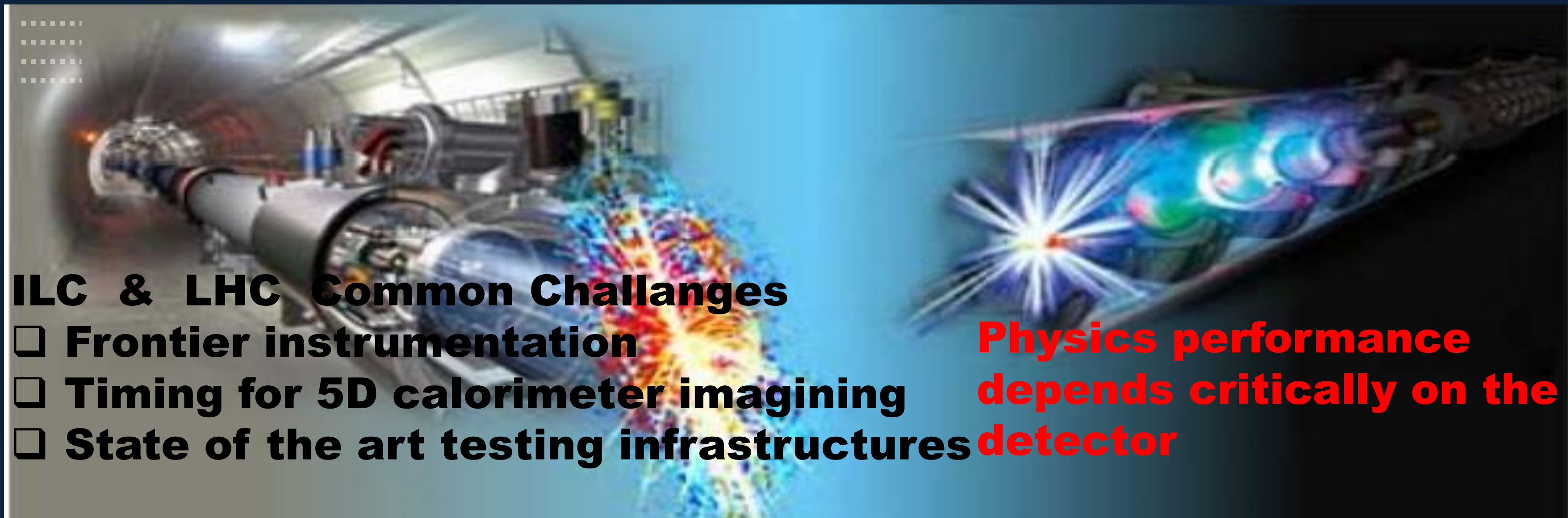

Our motivation to present the talk: sharing the knowledge we gained building and using the advanced testing infrastructure.

The synergy between the Large Hadron Collider and the International Linear Collider during concurrent running of the two machines has the potential to maximize the physics gain from both facilities.

- **Physics research**
- **R&D in technology innovations**
  - **5D calorimetry (x,y,z,E,t), particle flow calorimétrie, 4D tracking**
  - **Novel silicon sensors for high-precision 5D calorimetry (timing sensors: example - LGAD); Nice addition for ILC for PID**
  - **Experimental characterization tools for detectors R&&D (topic of this talk): 2D/3D imaging of sensors (TCT) for leakage current, CCE, timing performance study, breakown voltage**
  - **Many more ...**

Advancing testing infrastructures

With perpetual need for examining new sensor structures for dosimetry, calorimetry and particle tracking experiments, many techniques were developed during the last couple of decades, which make studies of both microscopic and macroscopic detector properties possible.

The conventional Transient Current Technique is a key tool for studying signal formation, charge collection and trapping mechanisms inside the semiconductor detector.

However, studies of segmented devices require very good position resolution of deposited charge for examining the position resolved charge collection properties in such detectors.

New advanced technique offers examining of complex structures, involving all types of position sensitive silicon detectors (pad, strip, pixel, 3D), as well as MOS structures.

As it will be demonstrated advanced fs-TCT platform ivecomes a powerful tool for breakdown voltage study.

Standard TCT

Standard (top) TCT – where the device is illuminated and examined from the top (either front or rear electrode). The depth of e-h pair generation depends on the wavelength of the light or energy and type of ionizing particle and of course on the semiconductor. In silicon for example, λ = 670 nm penetrates only a few microns, similarly alpha particles penetrate around 20 µm, while IR (1064 nm) penetrates a few millimetres, which is similar to the ionizing electrons from a radioactive source (e.g. 90Sr).

Edge-TCT – where the device is illuminated from the side by an IR laser, in which case the e-h pairs are created at a certain depth inside the structure. [6-8].

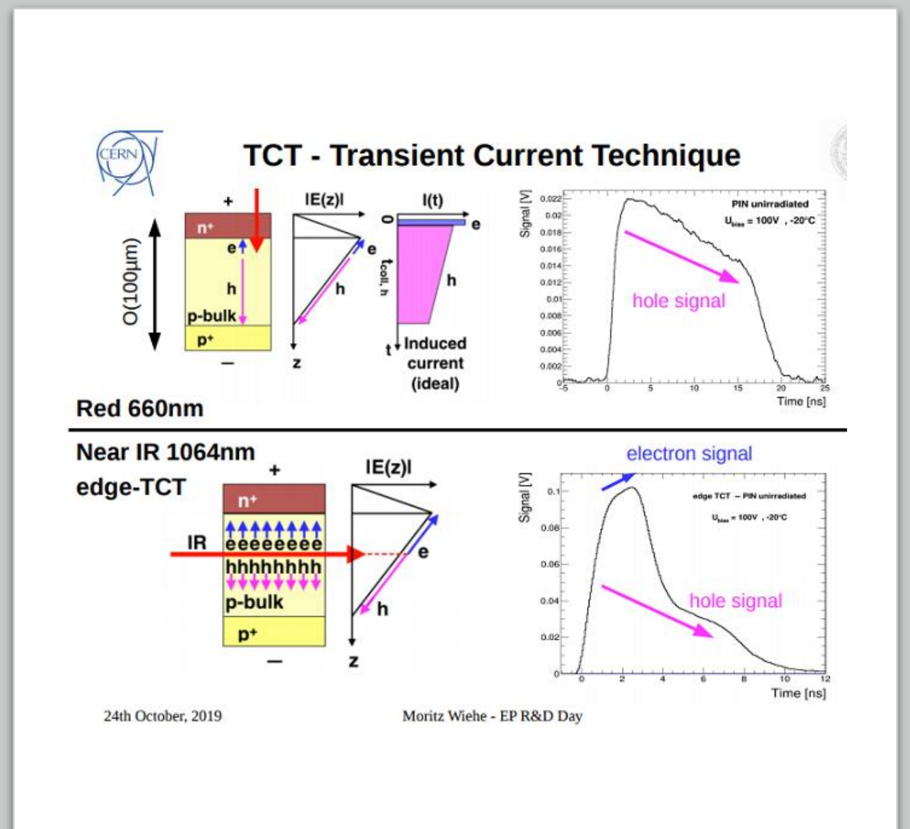

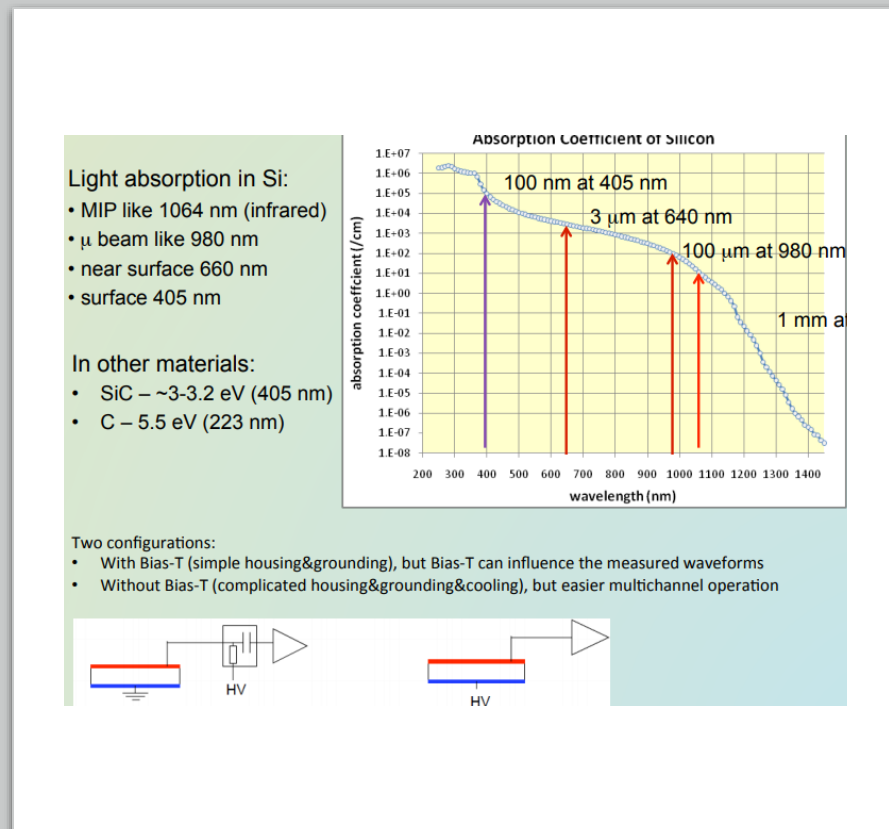

3D imaging

First table TCT-TPA developed at CERN

CERN-TPA laser system (CERN 186/R-G25)

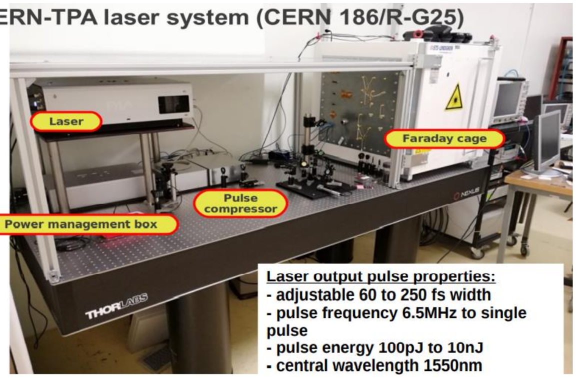

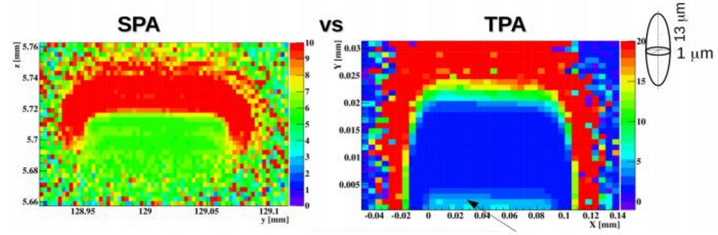

HVCMOS sensor
100 µm x 100 µm;
10 µm depleted;
Imaged by edge-TCT (left) and TPA-TCT (right|)

Moritz Wiehe – CERN - TPA-TCT, 36th RD50 Workshop

Concept firstly studied at the laser facility in Spain

Advantage of TPA: charge generation only at focal point – very good spatial resolution – 3D mapping of sensor

TPA laser facility

sgiker

- Measurements conducted at the Singular Laser Facility of the UPV (Bilbao, Spain).
  http://www.ehu.es/SGIker/es/laser/
- Very flexible and tunable laser system (intensity, λ, pulse duration...)
- Access granted via RD50 collaboration.
- See backup for full specs

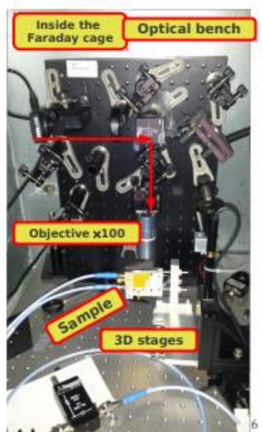

In this study:
λ=1300 nm, 12 nm bandwidth, Δt=240 fs

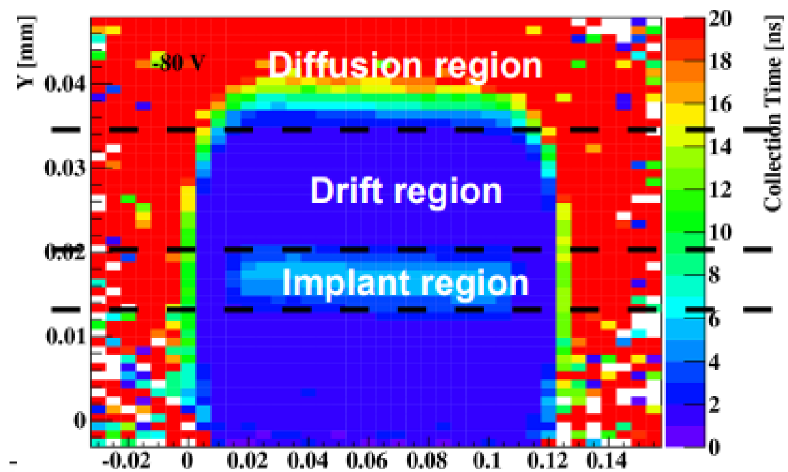

- Marcos Fernandez - 28th RD50 Workshop – June 2016, Torino (Italy)

Fs-TCT Set up at ELI : Motivation

To build unique fs-TCT with both lines, Single Photon Absorption at 800 nm the and Two Photon Absorption at the 1550 nm of fs-laser

Requirements for TPA-TCT:
- Sub band-gap energy laser
  λ > 1100nm (E < 1.12eV)
- **large enough intensity**

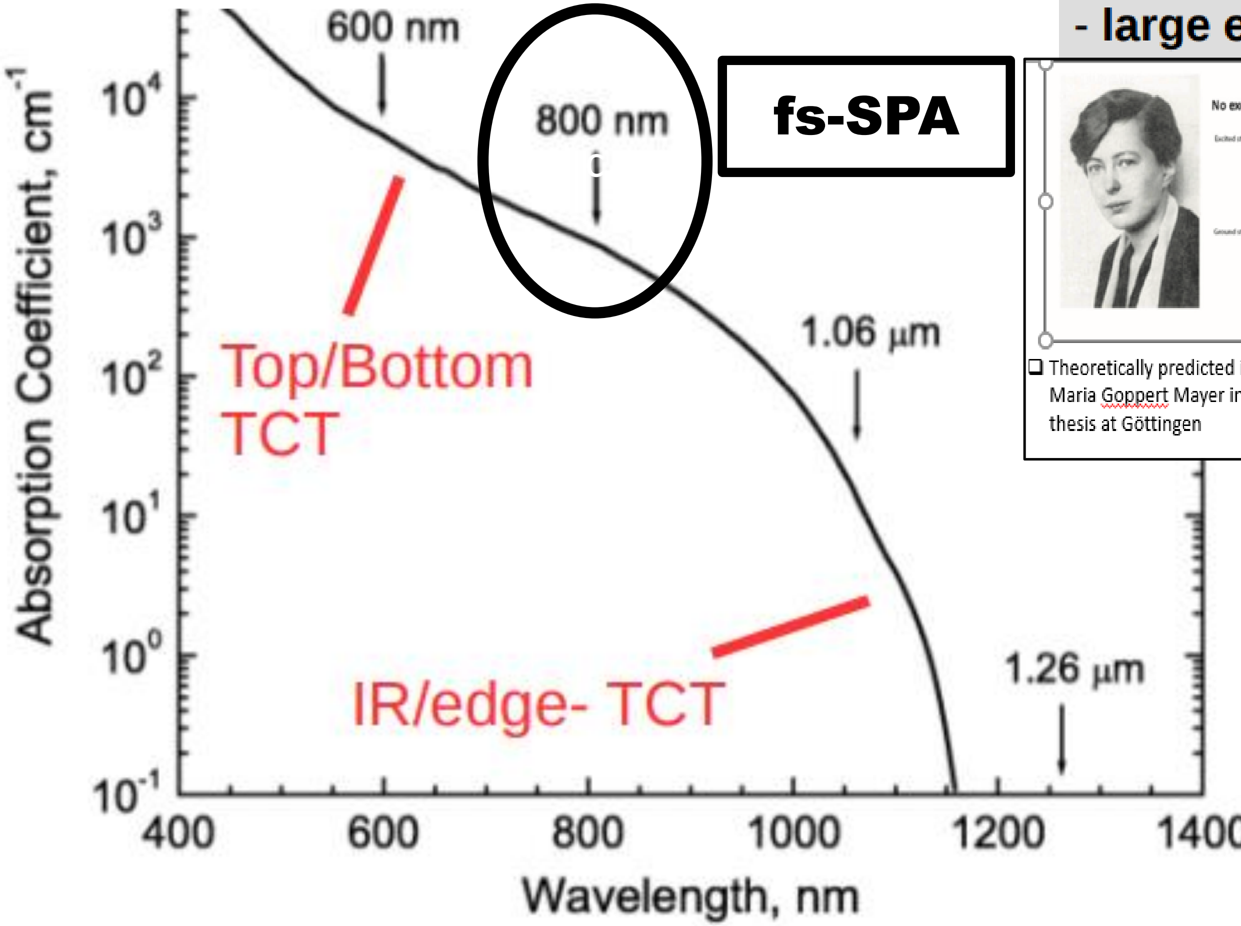

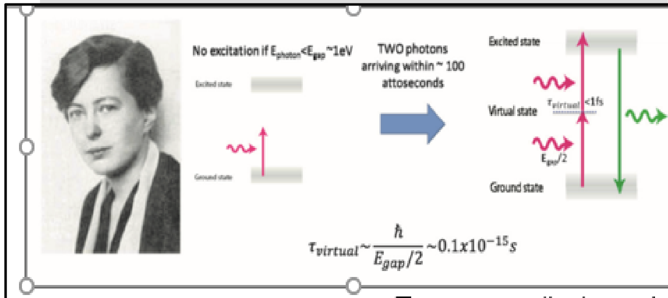

- ❑ Theoretically predicted in 1931 by Maria Goppert Mayer in her Ph.D. thesis at Göttingen
- ❑ Experimentally observed in CaF2:Eu2+ by Kaiser and Garret at Bell Labs in 1961

TPA-TCT
1550nm

Subbandgap Laser-Induced Single Event Effects:

SPA/TPA-TCT setup at ELI Beamlines

The world unique and powerful platform for sensor characterization and R&D research

ELI BioLab

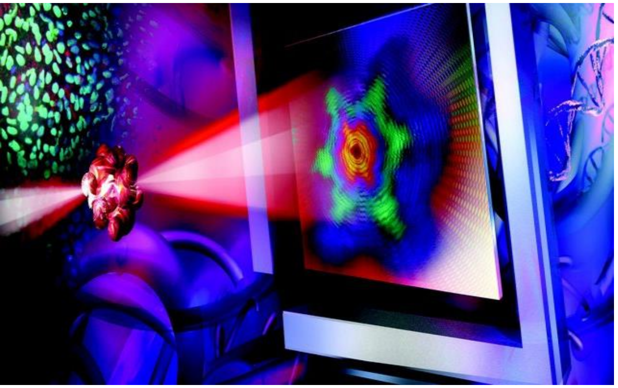

Experimental hall E1

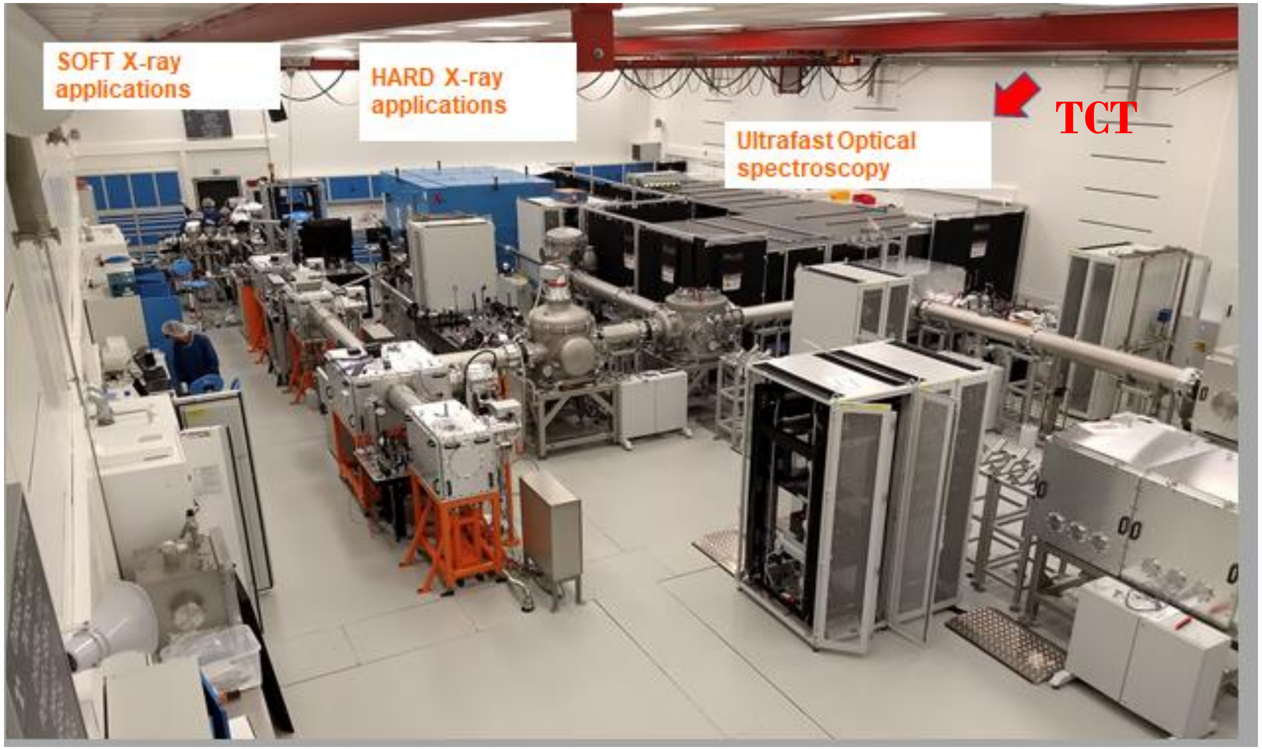

In collaboration with ELI Beamlines facility and ELI BioLab, the advanced fs-laser-based TCT/SPA-TPA infrastructure is developed.

3th TCT-TPA in the world
1st table TPA-TCT build at CERN

Project supported by: Advanced research using high intensity laser produced photons and particles (ADONIS)   Reg. n.: CZ.02.1.01/0.0/0.0/16_019/0000789

European Extreme Light Infrastructure (ELI Beamlines) in Dolní Břežany, CZ

The first laser research infrastructure world-wide which is the result of a coordinated effort of a multi-national scientific laser community. I.e. a sort of CERN but in the laser research field.
The main goal of ELI BL is to provide secondary sources (based on lasers) and world strongest lasers to users (1 PW, 10 PW). It also provides lower power fast fs-class lasers which we used.
www.eli-beams.eu

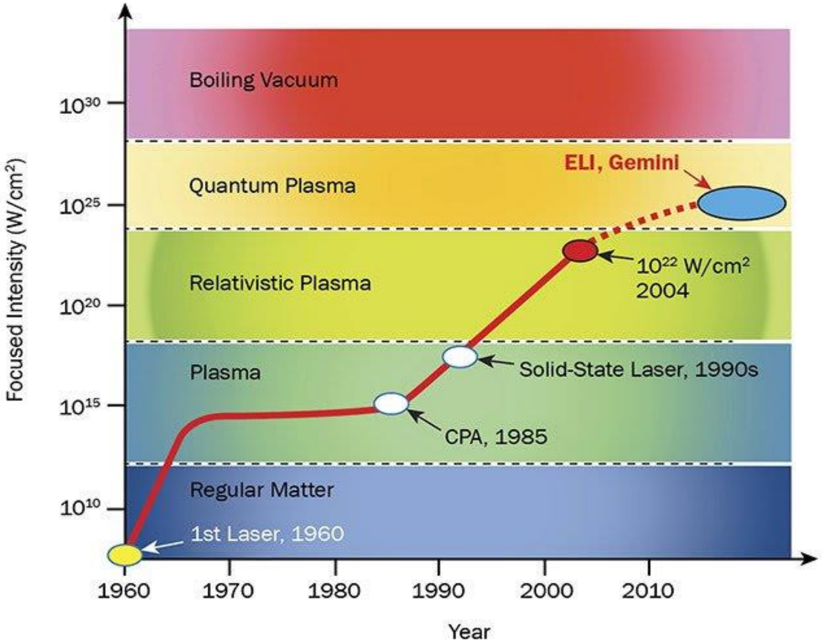

THE MOST RECENT RESULT: ELI BEAMLINES REACHED THE HIGHEST AVERAGE POWER EVER DEMONSTRATED BY A PETAWATT LASER!
Operation of the L3-HAPLS laser system (ELI Beamlines Research Centre) at 0.5 PW level was demonstrated through compression of the full energy output pulses currently generated by the laser chain, in the Petawatt vacuum compressor.

Schema for Experimental setup: **SPA** configuration

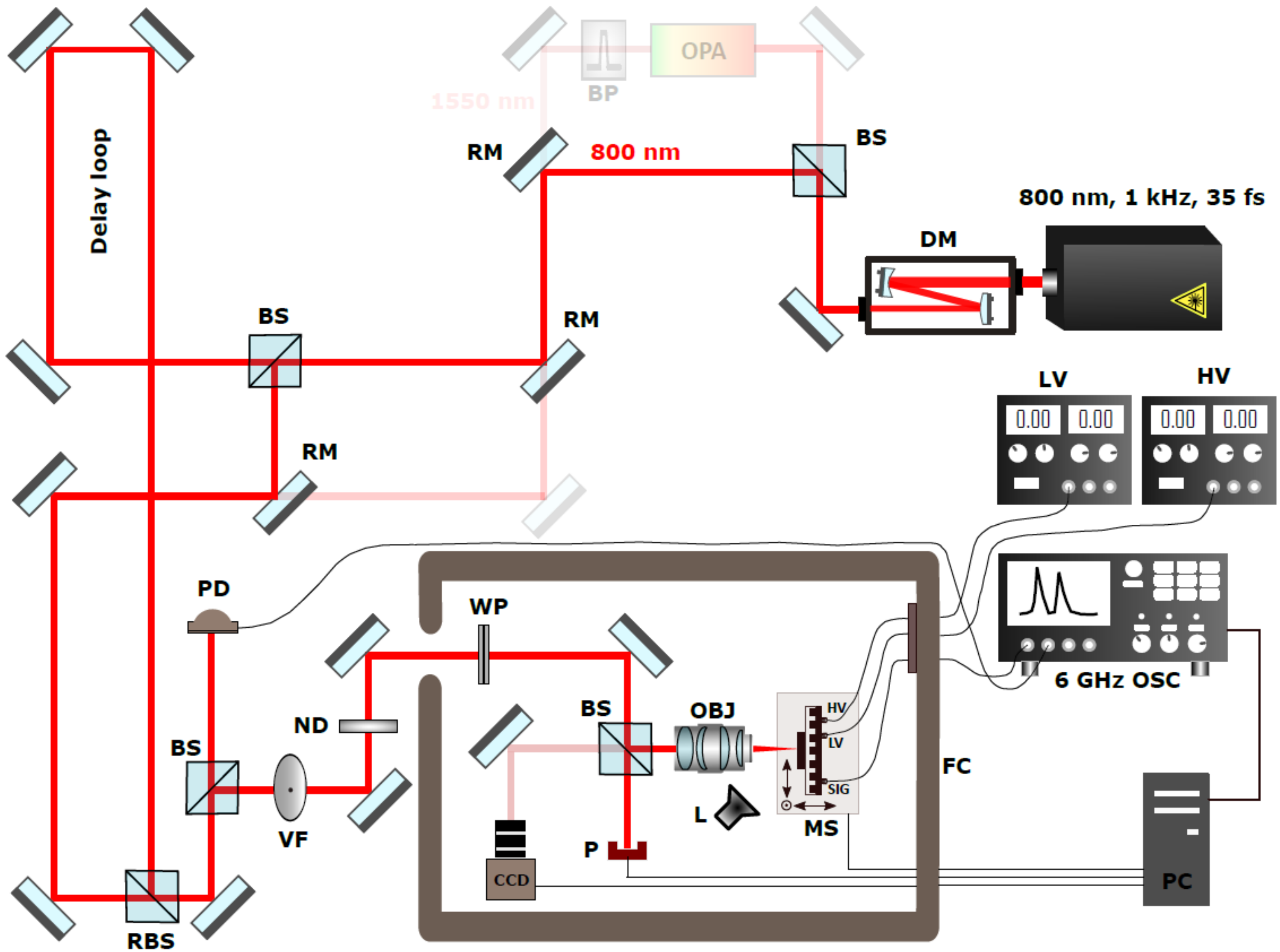

DM – demagnifier**, BS –** beamsplitter, **OPA -** optical parametric amplifier, **BP -** bandpass filter, **RM -** removable mirror, **RBS -** removable beamsplitter, **PD -** reference photodiode, **VF -** variable gradient ND filter, **ND -** fixed neutral density filter, **WP -** half waveplate, **P –** powermeter, **OBJ -** 100X objective **L-** lamp, **MS -** motorized XYZ stages, **LV -** low voltage power supply, **HV -** high voltage power supply, **FC -** Faraday cage

Experimental setup: **TPA** configuration

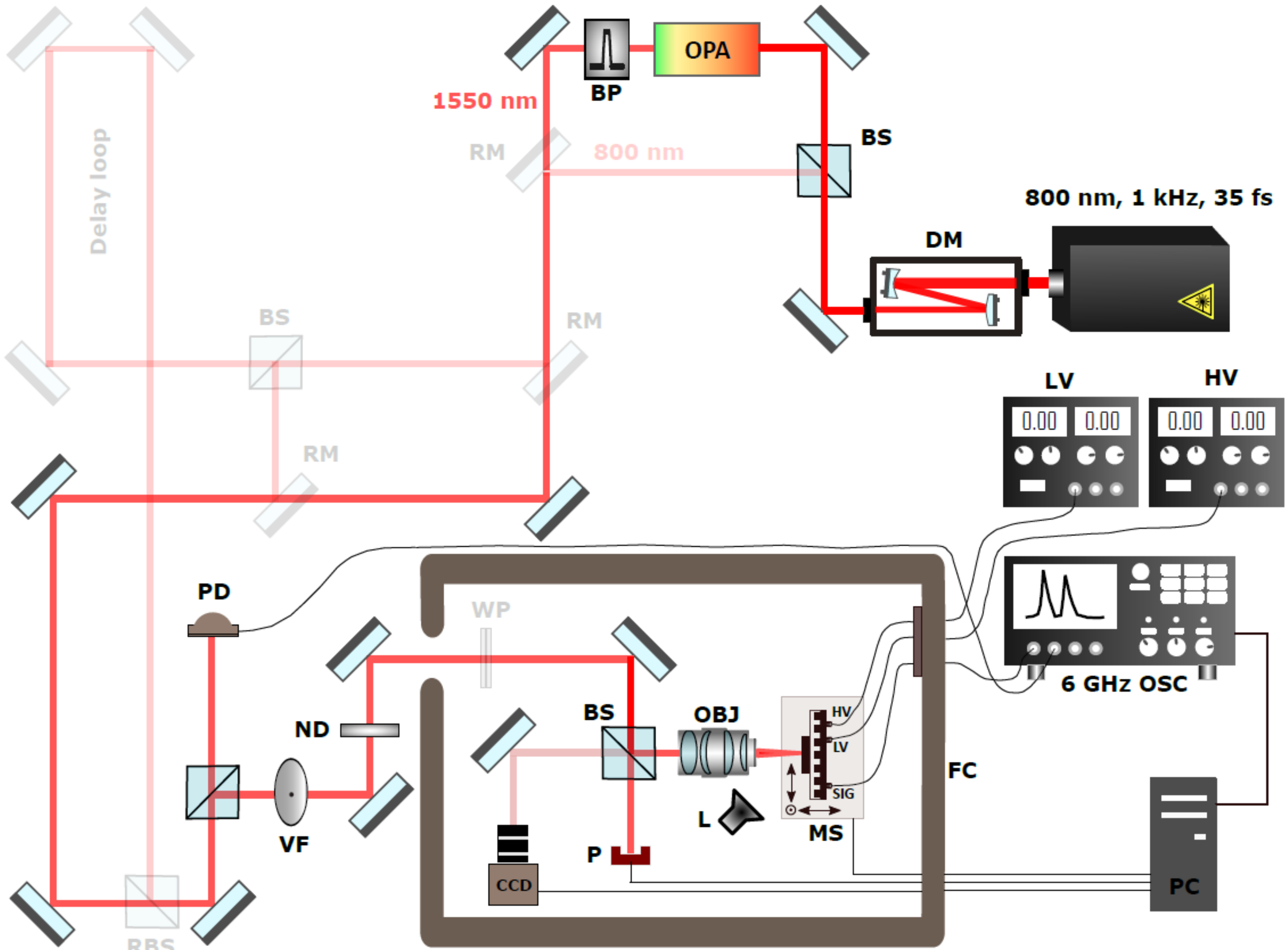

DM – demagnifier**, BS –** beamsplitter, **OPA -** optical parametric amplifier, **BP -** bandpass filter, **RM -** removabe mirror, **RBS -** removable beamsplitter, **PD -** reference photodiode, **VF -** variable gradient ND filter, **ND -** fixed neutral density filter, **WP -** half waveplate, **P –** powermeter, **OBJ -** 100X objective **L-** lamp, **MS -** motorized XYZ stages, **LV -** low voltage power supply, **HV -** high voltage power supply, **FC -** Faraday cage

TCT/TPA-SPA set up

Optical Parametric Amplifier TOPAS Prime and two table-top fs-lasers (Legend and Hidra) in BioLab

TCT-SPA/TPA set up

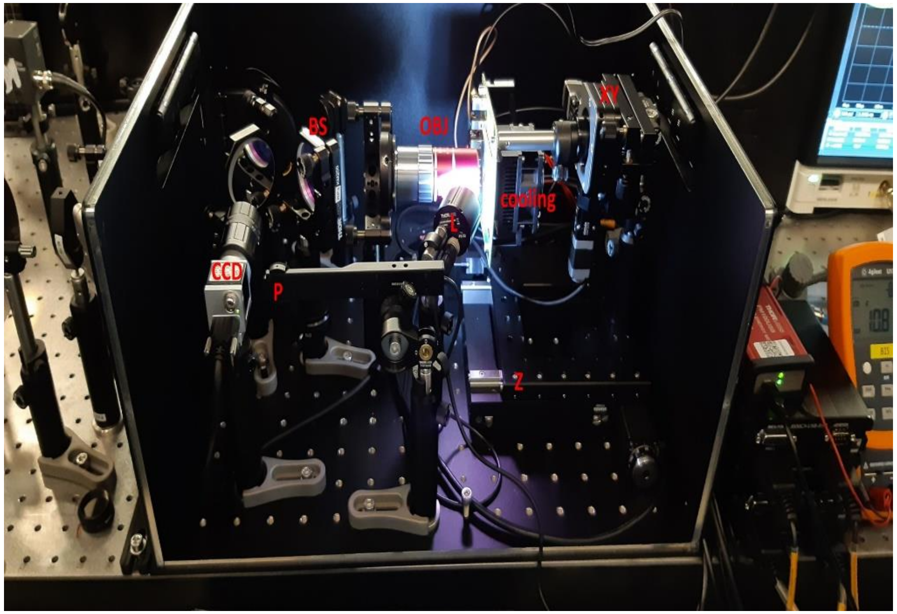

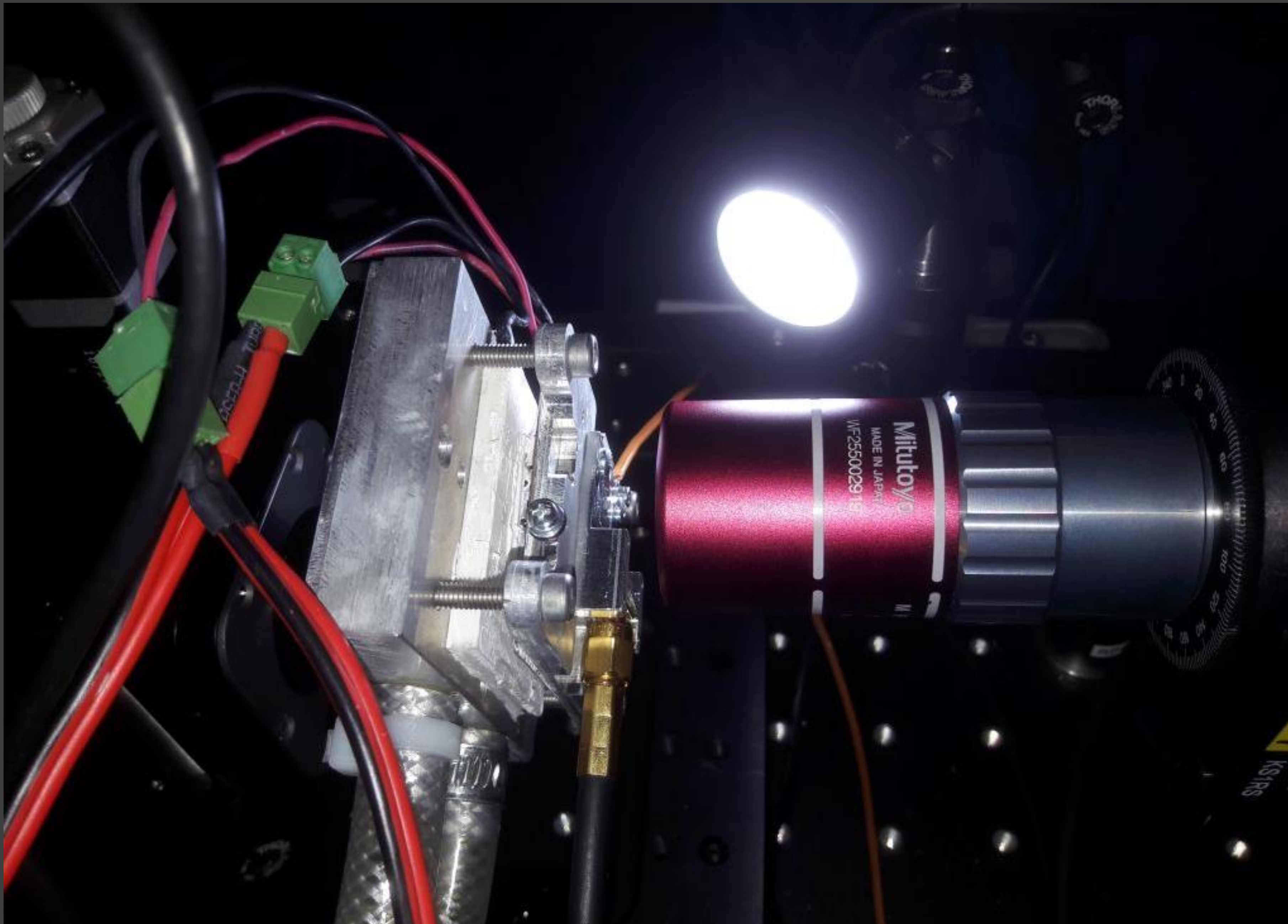
Mitutoyo

Beam waist parameter

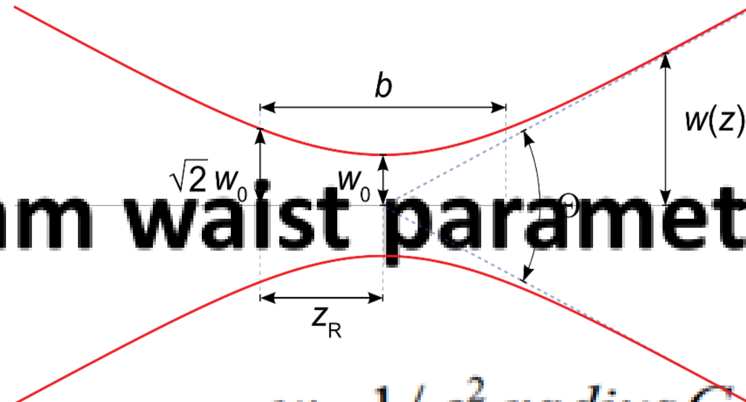

800 nm (SPA)

$$w - 1/e^2 \ radius \ Gaussian \ beam$$

$$P_{measured} = \frac{A}{2}\left[1 - erf\left(\frac{\sqrt{2(x-B)}}{w}\right)\right]$$

- **Rayleigh length is z_0=3.31 um.**
- **The waist** radius looks quite good **w_0=0.85 um.**
- **The beam diameter (1/e2) is 1.7 um** and this is actually limit of our resolution (stations are more precise).

All these data are for 800 nm

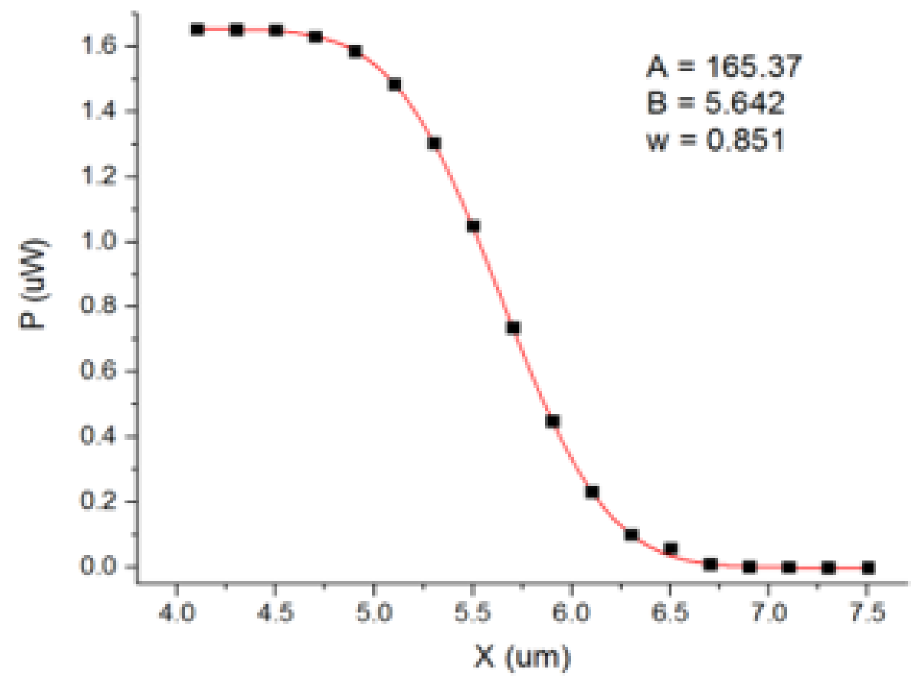

1550 nm (for TPA)

$$P_{measured} = \frac{P}{2}\left[1 - erf\left(\frac{\sqrt{2}(x - x_0)}{w}\right)\right]$$

$$w - 1/e^2 \ radius \ Gaussian \ beam$$

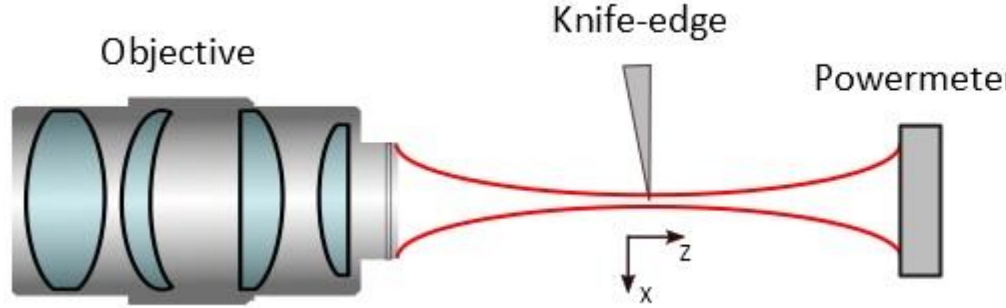

100X Mitutoyo Plan Apo NIR HR Infinity Corrected Objective
λ = 1550 nm

1. P(x) measured for series of Z points around focal point
2. w(Z) obtained by fitting for every Z
3. w_0 and Z_R obtained by fitting w(Z) curve

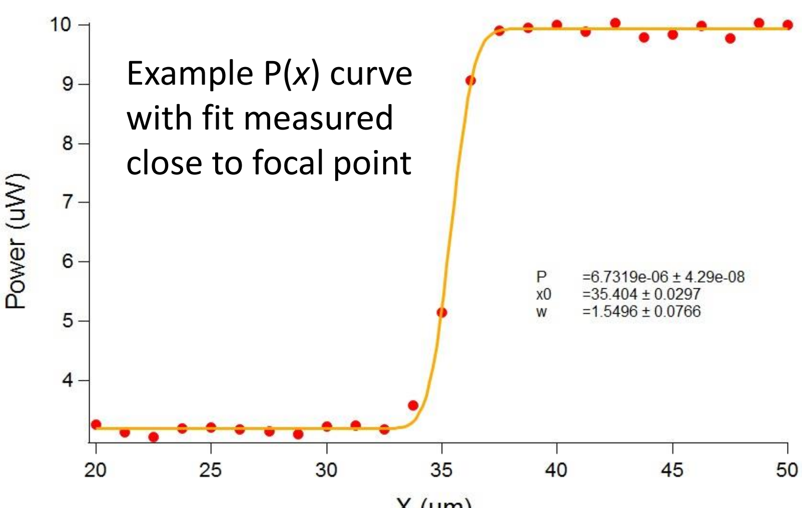

$$w(z) = w_0\sqrt{1 + \left(\frac{z - b}{z_R}\right)^2}$$

$$z_R - Rayleigh \ \ range$$

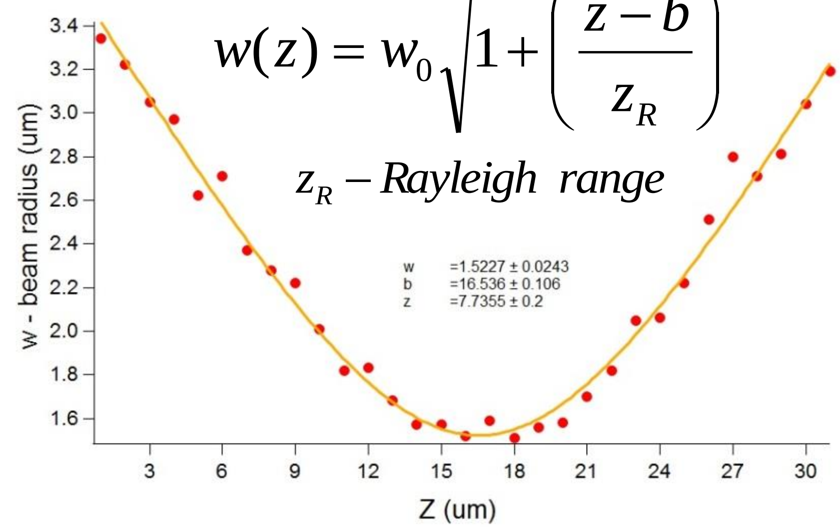

Final parameters (in air):
$w_0 = 1.52\ \mu m$
$Z_R = 7.74\ \mu m$

In Si : refractive index correction needed
$n = 3.48$ *at 1550 nm*

$NA = 0.31$ (nominal NA=0.7 but probably not valid for focal point)

Proof of TPA
LGAD WF25 (HPK-P2)

Signal ~ Irradiance^2

$$\frac{\mathrm{d}N(r,z)}{\mathrm{d}t} = \frac{\beta I^2(r,z)}{2\hbar\omega} \Rightarrow \Delta N(r,z) = \frac{\beta I^2(r,z)}{2\hbar\omega}\Delta t$$

$Q \propto N$ $\quad P \propto I$

- ❑ Quadratic relation between collected signal (in Si) and laser power

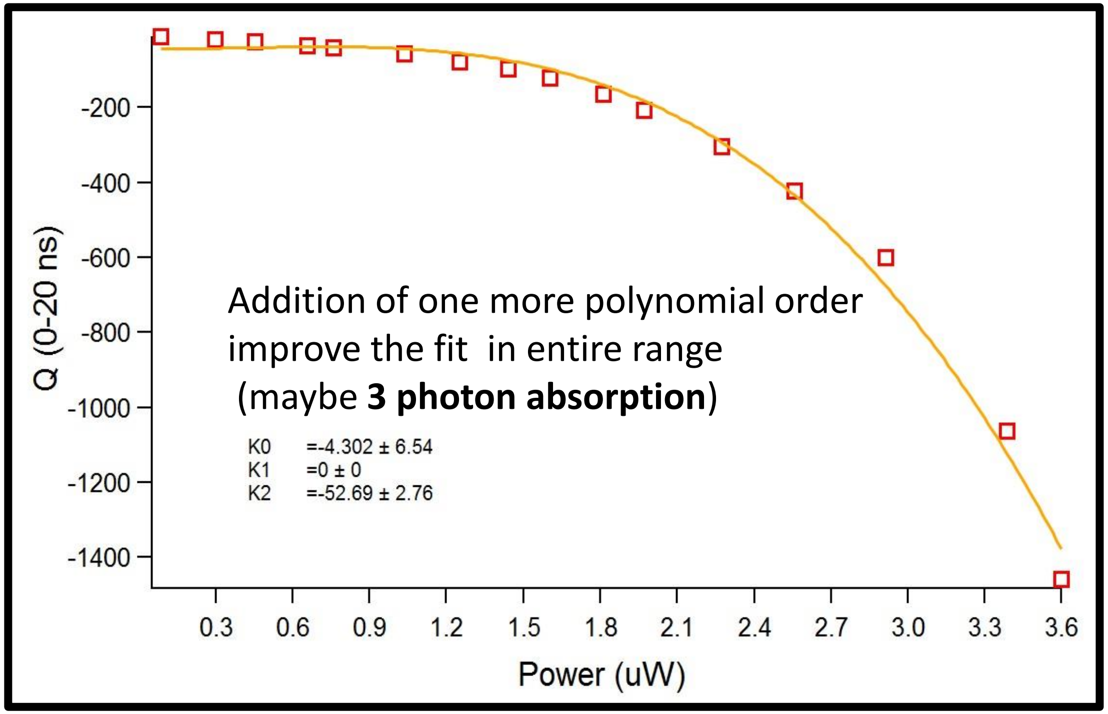

Our current research program

- **Study of mortality fatalities of the irradiated sensors at high pulses/Single Event Effect**
  - The fact that we can create lots of e-h pairs very fast makes our setup ideal to study mortality of the irradiated sensors at high pulses. At very high bias voltages ATLAS/HGTD detectors break down sooner at test beam than in the ^{90}Sr test bench.
    - The standard lasers are not fast enough to create so highly dense ionization both in time and space while ELI's is (e-h generation of the same speed as for particles, pulse energy can be increased to hundreds M e-h/pulse even higher than fragments of inelastic nuclear collisions that can be a reason)
    - The setup presented here is able to tune/change the wavelength (to a certain extent) and by that the penetration depth too.
- **Gain layer profiling with TPA and understanding the changes after irradiations**.
  - Impact ionization measurements (possible generation close to the edge of gain layer);
  - Understanding acceptor removal.
- **TPA and SPA studies of inter-pad region – understanding the edge**

Background:LGADs breaking down at high V_{bias}

- Destructive breakdowns appear mostly in the test beams (TB) – much less in the laboratory setups (Sr90, probe stations)
- HPK-P2 sensors seem to be robust in the laboratory conditions.
- Destructive breakdowns (fatalities) appear at bias voltages that are significantly (50 -100V) lower than those in the lab.
- They appear suddenly without a clear warning (increase of leakage current, instability in leakage current, changes in gain; this also seen in ELI tests)
- The reasons for these breakdown are not well understood:
  - Is it the high electrics field in highly irradiated sensors that is the problem?
  - Is it the gain of the devices that plays a role?
  - Is it the irradiations that are the reason, or they merely facilitate the conditions where high bias voltages can be applied?
- The main difference between lab (Sr-90 with E_{max}=2.3 MeV) and TB (up to several tens MeV deposits – CMS paper) is the energy of the particles:

  Can huge amount of charge in a single collision cause a conditions that lead to a destructive breakdown?

Ref/CMS paper: Mika Huhtinen, Highly ionising events in silicon detectors, CMS Note, March 2002

A possible explanation

Presented at TREDI2021

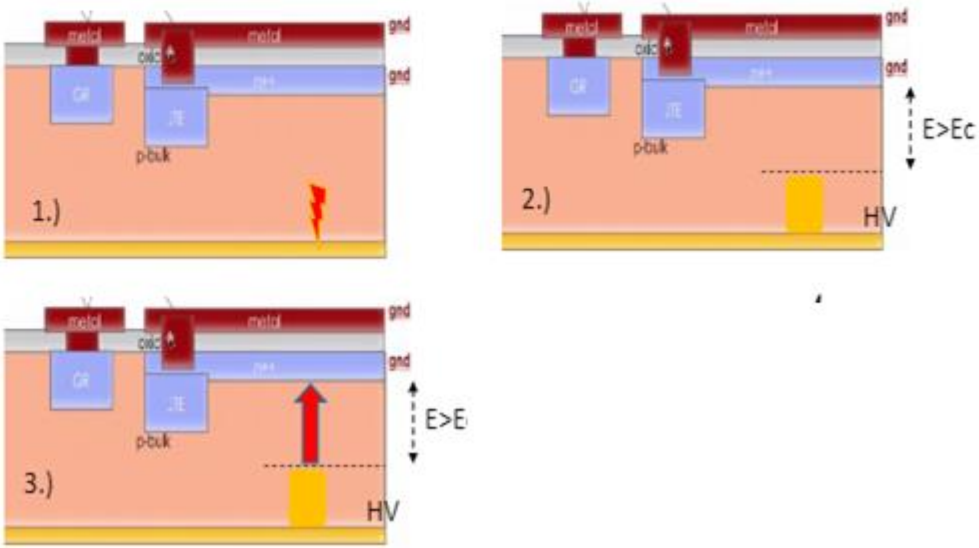

1.) larger deposition of the charge (fragments producing deposition in few um as large as 1000 mips- CMS tracker paper) in few um (not possible with lab sources)

2.)larger density of carriers leading to collapse of the field (screening prevents the carriers from being swept away

3.) once the field collapses the HV is brought closer to the pad which leads to very high field strength leading to avalanche breakdown and full discharge of sensors and bias capacitor

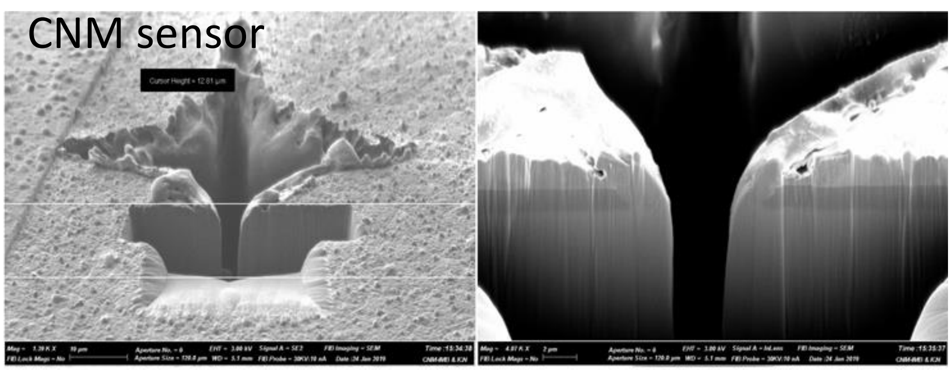

"courtesy of CNM (ATLAS TB sensor)"

Thanks to CNM for providing the photos of such fatality.

If the speed of deposition is similar to Mip then the laser test with extremely high energy per pulse in 50 fs should lead to fatalities
Tests uses 800 nm (27 μm penetration) of 50 fs pulses with pulse of up to a 1 mJ.
Pulses are focused to dimensions similar that of mip deposition (1-2 μm cone)

Fatality studies - samples and readout

- The samples are from HPK-P2 run, the latest ATLAS/CMS LGAD fabrication (shown in many talk in the workshop)
  - W36 (Vgl~51.5 V, Vbd~220 V)
  - fluences covered are the ones of interest for ATLAS and CMS: 4e14, 8e14, 1.5e15, 2.5e15 cm^{-2}
- For each sensor (4 sensor, 4 fluences) the bias was increased up to the maximal expected value (340, 520, 680, 780 V for respective samples) where the IV was measured

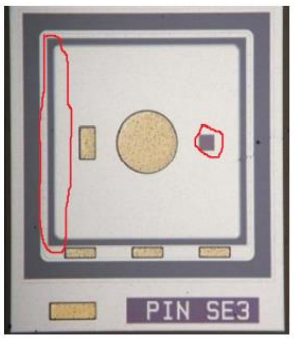

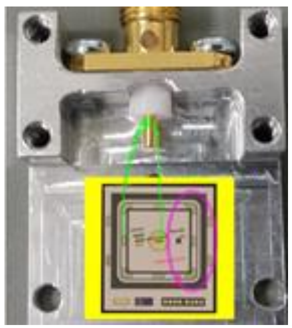

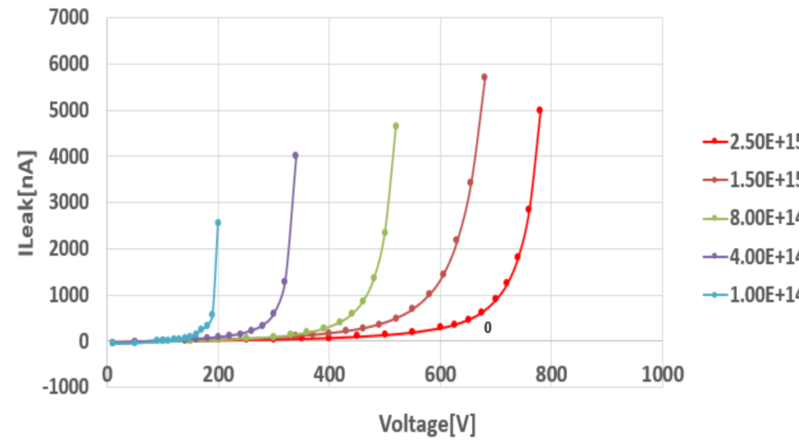

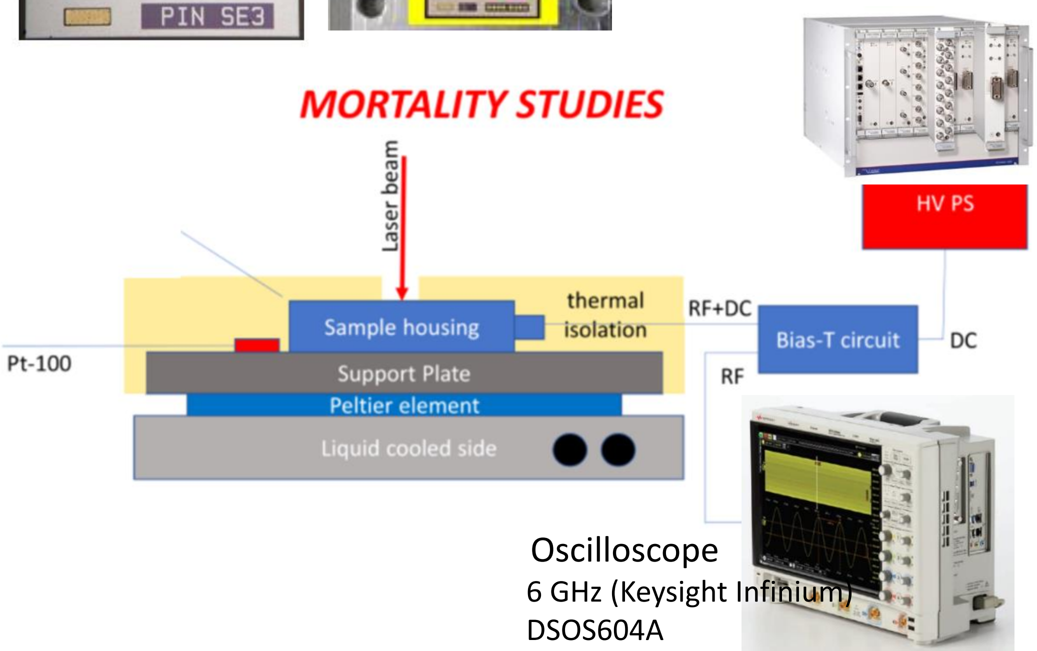

- Closed circuit chiller T=-25C
- N2 flushed to avoid condensation.
- No active amplifier used-we want large signals.
- Bias-T used to prevent discharge into oscilloscope
- No other bias filtering used
  - ✓ HV power supply: EB1200305040000200 (Iseg)

Example of Fatality Signature

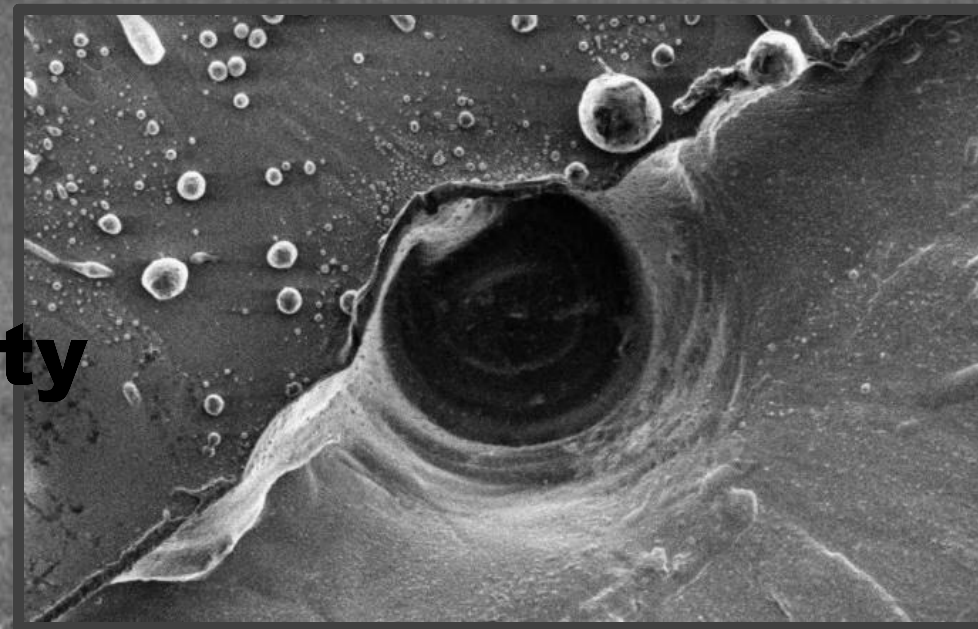

W36 LGAD 1.5e15 cm^{-2} (I exp)

- ✓ The HV was set to 680 V
- ✓ After 3 nW illumination at 680 V the sample broke down (~10 MeV od deposited energy).

Presented at TREDI2021

Reported at the TREDI2021, Gordana Lastovicka-Medin et al.

MEASUREMENTS (I) Fatality signatures

WF36 LGAD (II exp) 2.5e15 cm^{-2}

- ✓ The HV was increased in steps, and survival of sensor at each step (chosen HV) was tested by increase of laser power till sensor brake down.
- ✓ In this case the LGAD broke down at bias of 450 V at 6 μW.
- ✓ Sample was still operational at lower bias HV=230 V

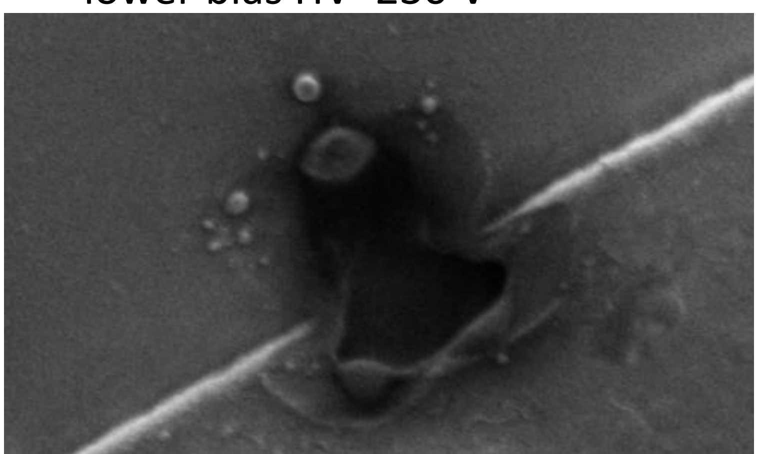

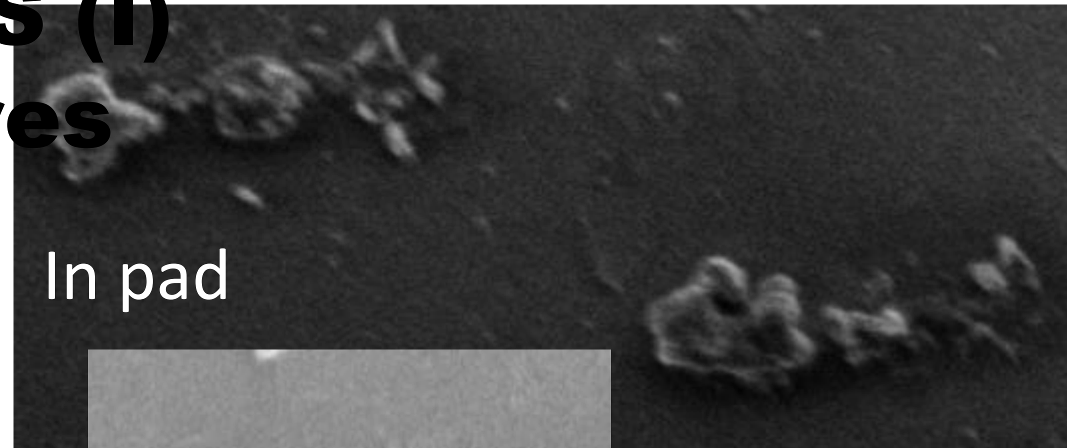

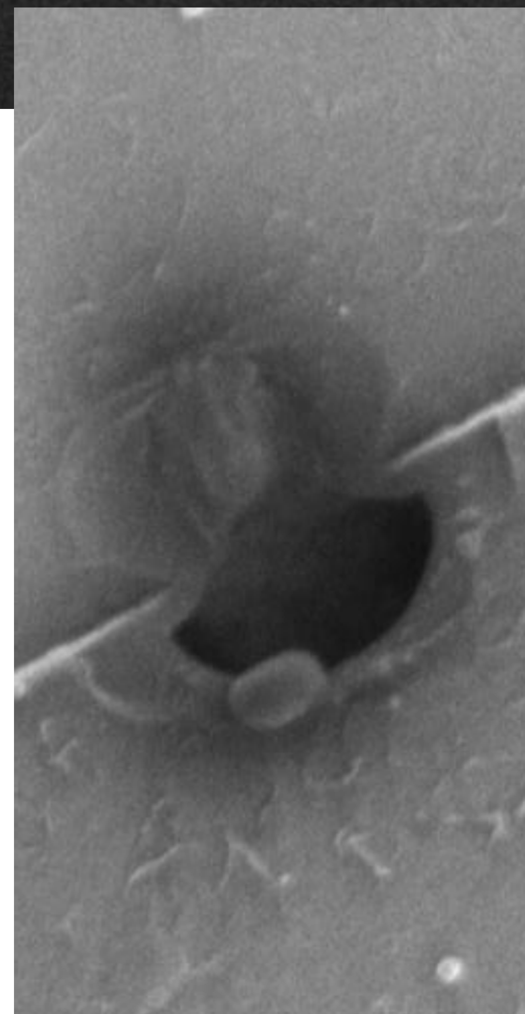

- Damage areas on the pad are clearly visible.
- Damage spots are also observed on the border of pad. It seems that this border region is especially sensitive to the damage.

Summery of results on fatality study

(reported at the TREDI2021) & Future steps

- We managed to set up extremely useful facility to study TCT with 50 fs laser of very high energies.
- The full setup can be operated cooled at ~-30^{o}C and flushed with nitrogen.
- We used 800 nm light with 50 fs pulses at 1 kHz focused in the centre of the LGADs and PINS from the latest HPK-P2 run irradiated to several different fluences 4,8,15,25e14 cm^{-2}.
- We focused our studies to establishing the conditions where sensors destructively break down:
  - ✓ It is clear that even highly energetic pulses, which produce more e-h pairs then theoretically possible at LHC, don’t destroy the sensors at <520 V
  - ✓ At higher bias voltages the amount of energy required is much smaller and 3pJ is enough at 680 V to destroy the sensors
  - ✓ Highest irradiated sensors can operate at 1pJ at 720 V – a much finer scan is needed to establish conditions
  - ✓ heating caused by the large breakdown current and high breakdown voltage causes the diode to be destroyed unless sufficient heat sinking is provided.
- It seems that all the fatalities occur at the metallization-opening interface!
- We will establish in the following campaign the voltage needed to break down the sensors using the beam pulse energy corresponding to approximately the maximum possible energies deposition by highly energetic particle interaction.
  - ✓ more work is required to full understand the mechanism (illumination spot is not where sensor breaks down) and establish the field/voltage where sensors break at e.g 5 pJ (approximately the maximum deposited energy in particle beams, correspond to 5 M e-h pairs).

Conclusion

- We established an interdisciplinary fs-laser-based unique technology platform to test and explore new frontiers in light and optics to build up new knowledge that could advance existing strategies for further silicon technology development, emphasizing LGAD timing sensors.

- In collaboration with ELI Beamlines facility and ELI BioLab, the advanced fs-laser-based TCT/SPA-TPA infrastructure will extend our ability to see the structures and signatures of LGAD fatalities in test beams and to pave the path towards mitigation of the underlying mechanisms causing these fatalities.

- Furthermore, it will also help to define the upper limits for critical bias working conditions and safe regime at the extreme fluences (LHC-HL, FCC) and lower fluences (ILC, CLIC). Here we presented an overview of the project aiming to set new testing strategies supporting further LGAD (heat sinking, JTE structure implementation and reverse engineering).

- Further utilisation of TPA will contribute further towards::
  - The understanding the sensor's response at the edge and between pixeled readout pads (important also for ILC)
  - The breakdown voltage is a key parameter of power devices. But, the breakdown of sensor devices is equally important as one typically reduces the device dimensions without reducing the applied voltages, thereby increasing the internal electric field.

We believe that R&D of detectors for both, ILC and LHC, will benefit from further exploitation and utilisation of the presented TCT-TPA/SPA testing station at ELI.

Thank you.

BACKUP SLIDES

Beam focused to the center of the sensor

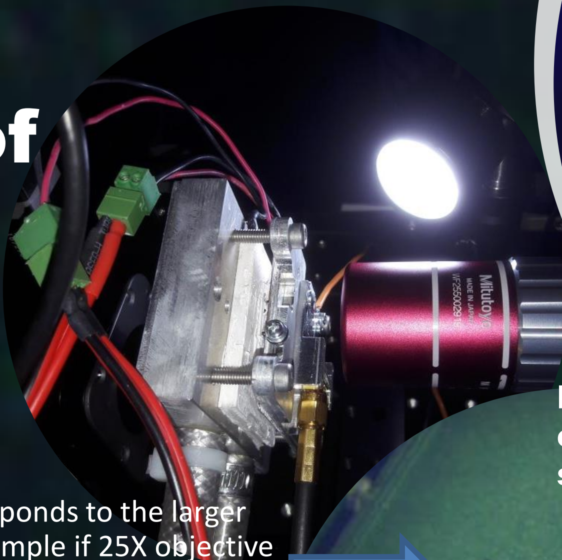

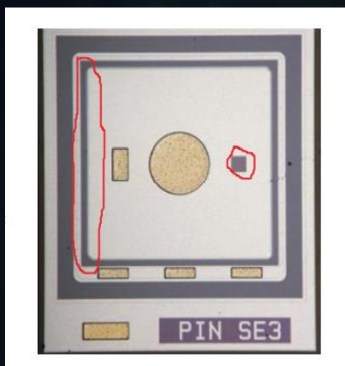

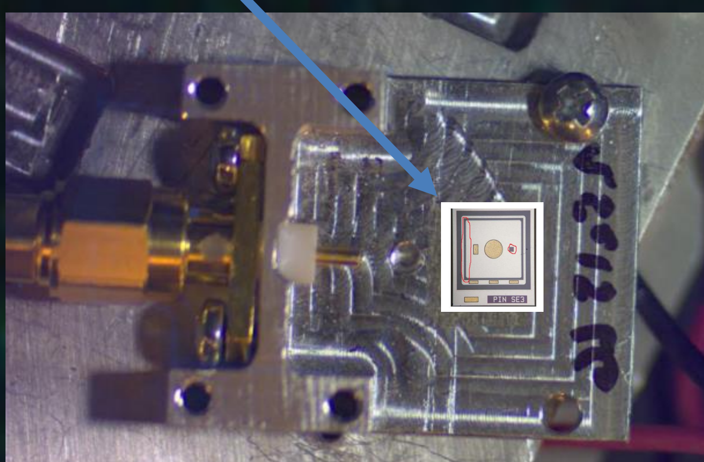

Image corresponds to the larger area of the sample if 25X objective is used instead of 100X (not used during experiment but used in pre-alignment of the sample position).

Pad of LGAD visible by imaging system

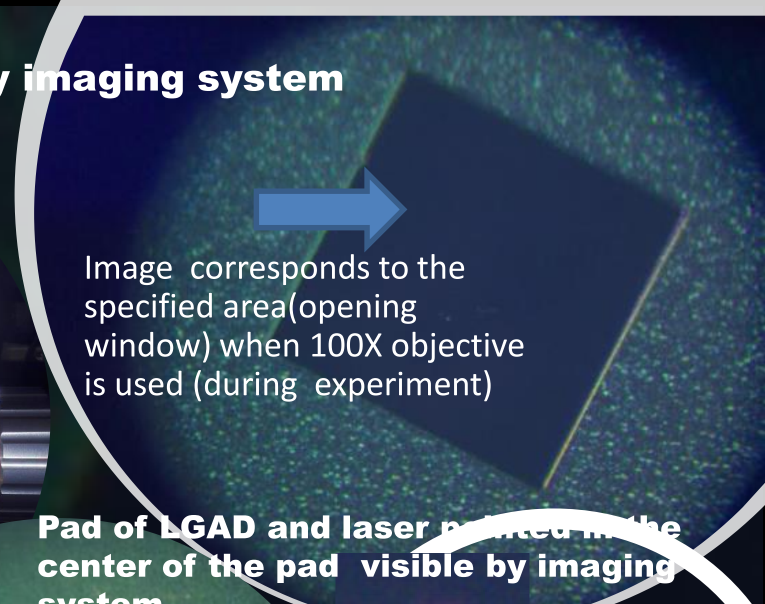

Image corresponds to the specified area(opening window) when 100X objective is used (during experiment)

Pad of LGAD and laser pointed in the center of the pad visible by imaging system

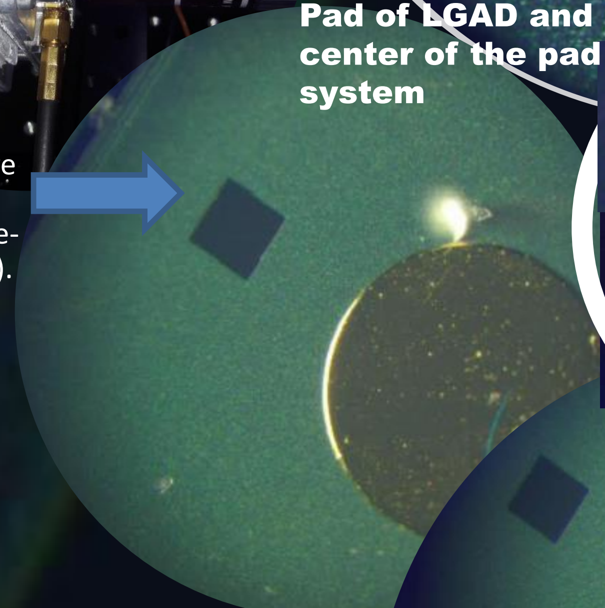

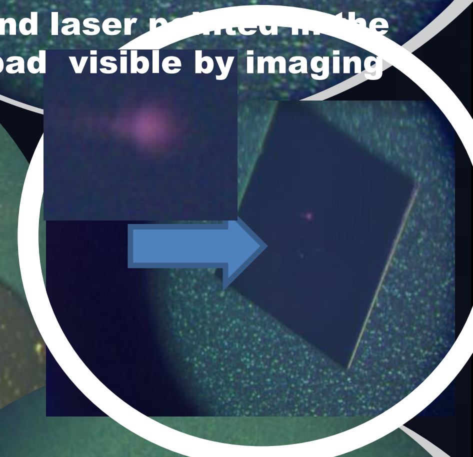

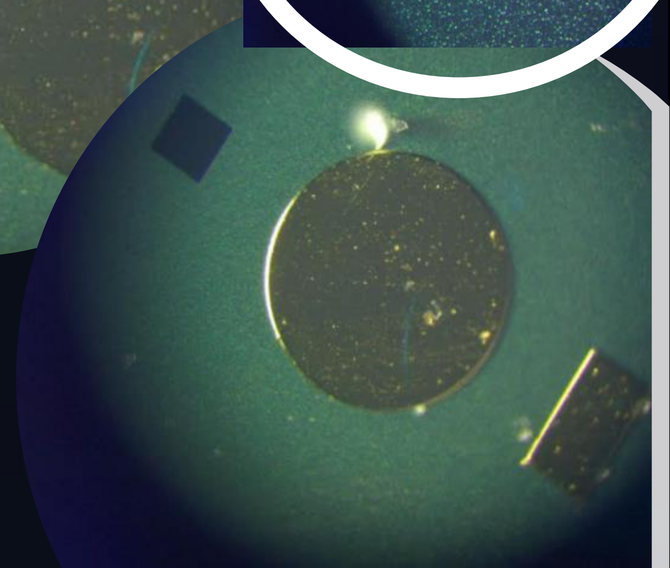

Comments (set up):

- setup contains a few removable elements on magnetic mounts to quickly change between 800 nm and 1550 nm beam
- for 800 nm optional half wave plate is used to flip polarization (the same S-polarization (vertical) is kept for all measurements)
- beam splitter in the front of objective is exchangeable, different ones are used for 800 and 1550 nm to give 50/50 split in both cases
- power is measured after the beam splitter (it enables constant monitoring of power during measurements)
- at 1550 nm power is measured by S132C Thorlabs power meter
- at 800 nm power is measured by PD300 Thorlabs power meter (much more sensitive at this wavelength
- if the most sensitive power meter is not enough in SPA (that was the case in mortality study where pW power gives already high signal) the additional ND filter OD=1 is insert in the front of objective (the actual power is attenuated by factor 10 in comparison to measured value)
- InGaAs reference diode is used to correct the laser fluctuations (it's important especially for long measurements: for xy scans for example) and to trigger the scope
- CCD camera with imaging lens (plus illuminating lamp) monitor when exactly we shoot. This system is used to precisely align position of detector and then is off (in principle illuminating lamp is off) during measurements

TCT signals

LGAD WF36, 4e14 n_{eq}/cm^2
P_{laser}=10 nW

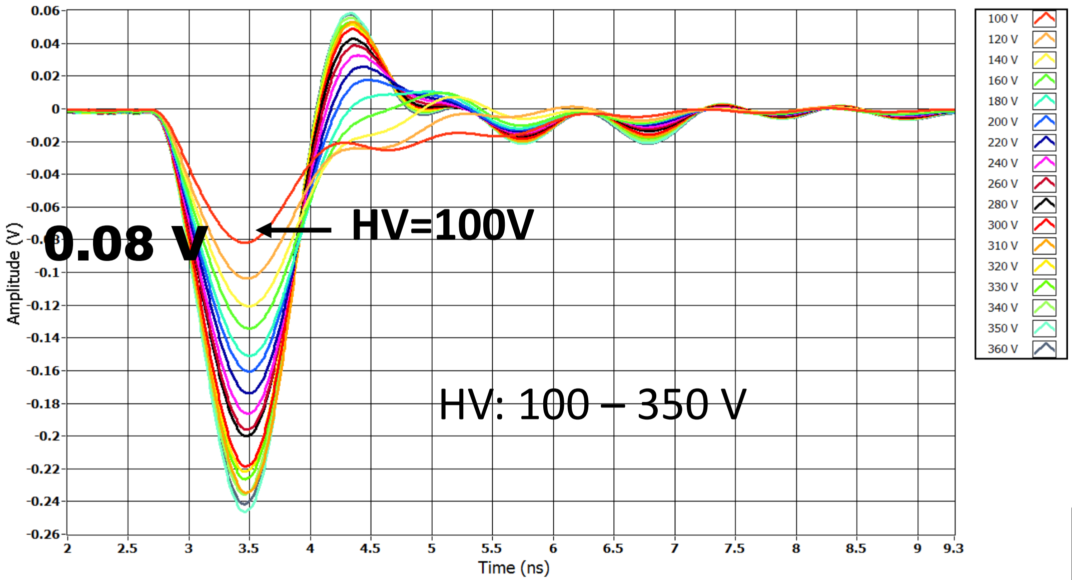

Generated Ne-h

1. Calculation from signal recorded on the diode at 10 nW

$$N_{e-h} = \frac{1}{e_0 R}\int_0^{5\ ns} V_{sig}(t)dt$$
$$N_{e-h} \sim \frac{1}{1.6e-19\ As\ 50\Omega} 0.08\ V\ \cdot 1ns \sim\ 10^7\ e-h$$

2. Calculation from the beam parameters at 10 nW

$$E_{pulse} = \frac{P}{\nu}$$
$$N_{e-h} = \frac{E_{pulse}}{e_0} \cdot Q_E\ \cdot R_{e-h}$$
$$N_{e-h} = \frac{10nW}{1000s} \cdot 0.5\ \cdot 1\ \cdot \frac{R_{e-h}}{1.6e-19\ As} = R_{e-h}\ \cdot\ 6.2\ \cdot 10^7\ e-h$$

3. A factor of 6 difference implies to large recombination possible. Recombination rate R is very much affected by the irradiation on. In order of both calculations to agree R has to be 1/6

4. The equivalent lost charge in the silicon to produce the same signal: $\Delta E = N_{e-h}\ 3.62eV =\ \sim 30\ MeV$

This is of the same order as seen in CMS paper(

Ref/CMS paper: Mika Huhtinen, Highly ionising events in silicon detectors, CMS Note, March 2002,

Exposure to extreme energies

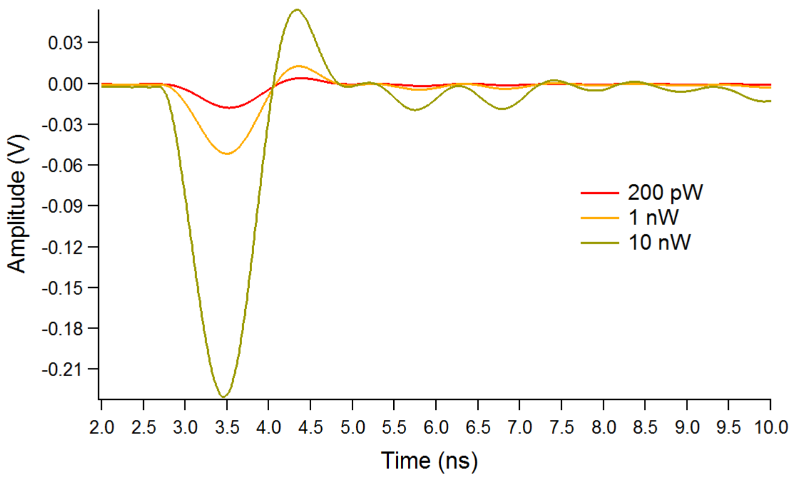

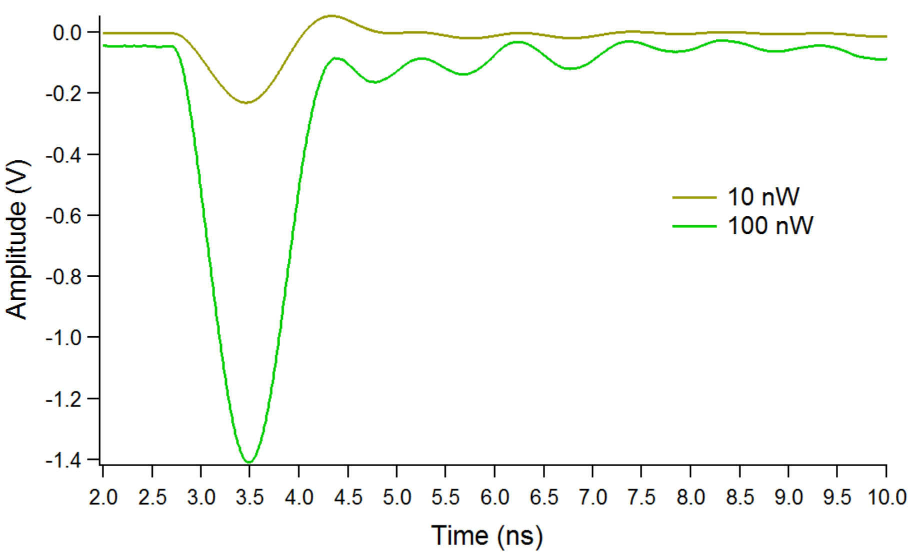

- ✓ WF36,
- ✓ 4e14 n_{eq}/cm^2
- ✓ HV was set to maximal HV (HV=320 V)
- ✓ Laser power was increased until LGAD died
- ✓ Changes in the signal waveform were observed
- ✓ Laser power L_{power} = 100 µW was critical point which completely destroyed the sensor
- ✓ P_{laser} = 100 µW is extremely large power; LGAD will never worked under such extreme power.

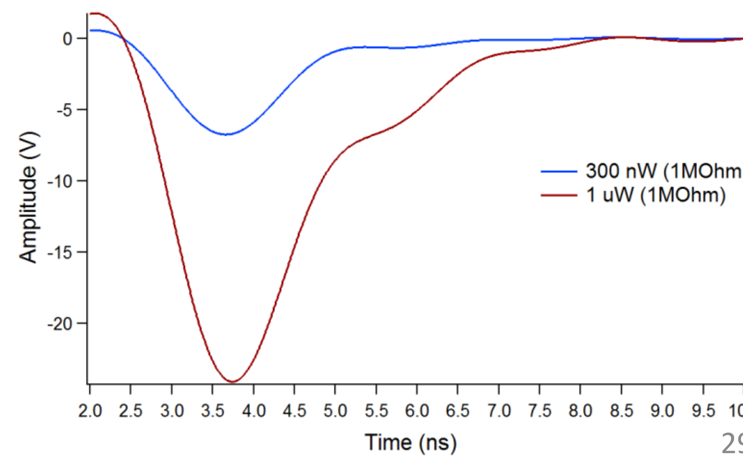

Parameter	Unit	LHC	HL-LHC	HE-LHC	FCC-hh
E_{cm}	TeV	14	14	27	100
Circumference	km	26.7	26.7	26.7	97.8
Peak $\mathcal{L}$, nominal (ultimate)	$10^{34}\text{cm}^{-2}\text{s}^{-1}$	1 (2)	5 (7.5)	16	30
Bunch spacing	ns	25	25	25	25
Number of bunches		2808	2760	2808	10600
Goal $\int \mathcal{L}$	ab^{-1}	0.3	3	10	30
σ_{inel} [331]	mb	80	80	86	103
σ_{tot} [331]	mb	108	108	120	150
BC rate	MHz	31.6	31.0	31.6	32.5
Peak pp collision rate	GHz	0.8	4	14	31
Peak av. PU events/BC, nominal (ultimate)		25 (50)	130 (200)	435	950
Rms luminous region σ_z	mm	45	57	57	49
Line PU density	mm^{-1}	0.2	1.0	3.2	8.1
Time PU density	ps^{-1}	0.1	0.29	0.97	2.43
$dN_{ch}/d\eta\|_{\eta=0}$ [331]		6.0	6.0	7.2	10.2
Charged tracks per collision N_{ch} [331]		70	70	85	122
Rate of charged tracks	GHz	59	297	1234	3942
$<p_T>$ [331]	GeV/c	0.56	0.56	0.6	0.7
Bending radius for $<p_T>$ at B=4 T	cm	47	47	49	59